ENGINEERING MECHANICS 2009
National Conference with International Participation
Svratka, Czech Republic, May 11 – 14, 2009
pp. 585–599
Paper #224

SURFACE ROUGHNESS AND EXTERNAL FLOW TURBULENCE JOINT EFFECT ON TURBULENT BOUNDARY LAYER

P. Jonáš*, O. Mazur, V. Uruba

Summary: *The individual and joint effects of surface roughness and external flow turbulence on turbulent boundary layer were experimentally investigated in the closed circuit wind tunnel IT AS CR. Fundamental mean flow characteristics were measured in turbulent boundary layers either on a smooth plate or on the plate covered with the sandpaper (80- grits) under turbulent flow with the intensity of almost isotropic fluctuations from the natural value, of about 0.003 up to 0.05 and with the relevant length parameter from 2.2 mm up to 30.5 mm .*

1. Introduction

Very often in engineering applications and environmental flows, the flow over a solid surface is turbulent and simultaneously the surface is rough. Numerous investigations were published on the individual effects of the rough surface or external turbulent flow on the flow in a wall layer (examples e.g. Jonáš, 2008). It appears surprising that the Authors did not found a paper devoted to an investigation of the joint action of the mentioned effects on a boundary layer flow (Jonáš et al., 2008). So, a preliminary study of the joint effect on turbulent boundary layer in a zero pressure gradient flow is the aim of this contribution. It is beneficial briefly remind the main consequences of the surface roughness and the outer turbulent flow on the turbulent boundary layer.

The flow in the wall region is controlled by the wall shear stress τ_w and the wall roughness characterized by the representative length (height) s of the roughness elements. The length s denotes e.g. the maximum hight of the roughness grains that generate wakes operating as sources of vorticity in the inner layer. The effect of surface roughness on the boundary layer is determined by the ratio

$$s^+ = \frac{s}{\delta_v} \tag{1}$$

where δ_v indicates the viscous length scale

$$\delta_v = \frac{\nu}{u_\tau}; \quad u_\tau = \sqrt{\frac{\tau_w}{\rho}}; \quad \tau_w = \mu\left(\frac{\partial \bar{U}}{\partial y}\right)_w \tag{2}$$

here μ, ν and ρ denote molecular viscosity, kinematics viscosity and density of fluid, $\tau_w(x)$ and u_τ are the local wall shear stress and the friction velocity.

* RNDr. Pavel Jonáš, DrSc., Oton Mazur, prom. fyz.,.Doc. Ing. Václav Uruba, CSc.: Institute of Thermomechanics AS CR, v.v.i., Dolejškova 5; 182 00 Praha 8; tel.: 20.266 052 025, fax: 420.286 584 695; e-mail: jonas@it.cas.cz

The flow is developing as on a *hydraulically smooth* surface if the roughness grains are nest in the viscous sub-layer, $s^+ < 5$ and the surface behaves as *completely rough* with grains overhanging the buffer- layer $s^+ > 70$. Further increase of roughness elements dimension s does not cause additional qualitatively changes of the flow. *Transitional roughness* region ranges between the above mentioned extreme cases

$$5 \le s^+ \le 70 \qquad (3)$$

The effect of roughness is namely in decreasing the viscous length scale δ_v and in a vertical shift of the mean velocity profile from the level of the roughness spikes, $y' = 0$, inside the layer of roughness grains, on the level $y' = -y'_0 \le 0$. A deeper analysis is given in e.g. Rotta (1962) and (1972), Pope (2000), Schlichting & Gersten (2000), Jonáš et al. (2008).

The turbulent boundary layer perturbed by outer flow turbulence is an example of the complex flows in the Kline et al. (1982) sense. The fundamental difference between a canonical turbulent boundary layer on a smooth wall in non-turbulent stream and the boundary layer under equal conditions except for the external turbulence comes from the fact that the turbulent outer stream is three dimensional and rotational in time and space. Therefore both molecular and turbulent diffusions are passing through the interface between the layer and the surrounding turbulent flow. The reasons for the existence of the Corsin´s super-layer disappear. Owing to this the fluid particles from the interior of the layer driven by the large scale motions penetrate deeper into the surrounding turbulent external flow and on the contrary, the outer flow particles - *turbulent eddies* – are entrained into the layer nearer to the wall. Turbulent diffusion across the layer amplifies. This has an impact on the increase in the friction velocity. The external turbulence is indistinguishable from the turbulence generating inside the layer provided that the external flow velocity fluctuations are not too large by comparison with the friction velocity. Thus the external turbulence does not affect the universal features of the mean flow in the inner region (e.g. Hancock, 1980) and its effect appears namely in thickening the layer and altering the velocity defect law in the outer layer.

Combining notions on the individual effects of wall roughness and external turbulence on turbulent boundary layer one must expect that their joint effect will appear across the whole layer.

2. Experimental facility and measurement technique

The flat plate boundary layer (*grad* $P_e = 0$) was investigated experimentally in the close circuit wind tunnel (0.5 x 0.9) m^2 in the Institute of Thermomechanics CAS, Prague. The boundary layer develops on an aerodynamically smooth plate (2.75 m long and 0.9 m wide) made from a laminated wood-chip board 25 mm thick in the primary configuration. Covering the primary plate with the 80-grit sandpaper on a thin plywood plate (7 mm thick) modifies the wall roughness. The rough plate leading edge has an elliptic shape (a x b = 60 x 20 mm^2) covering the primary leading edge. Presented results relates to the mean flow velocity from about 3 m/s up to about 15 m/s over either the smooth surface or the rough one (80-grit sandpaper with the maximum size of grains s = 0.343 mm ± 0.009 mm) and to the section 1.2 m downstream from the leading edge of plates.

The orthogonal clockwise coordinates system [*x,y,z*] is introduced with the coordinate x in the streamwise direction and the coordinate y in the direction of the outer normal to the wall. The zero x is in the leading edge plane (y, z) and the plane $y = 0$, the zero level, is the plane where the mean flow velocity equals zero, $U = 0$. The zero level lies on the wall in case of an aerodynamically smooth surface. The introduction of an auxiliary coordinate y' is proper with

$y' = 0$ in the top plane of the roughness elements in case of the rough wall as the velocity zero level is below this plane.

The features of the free stream turbulence (FST) were controlled by means of square mesh plane grids – screens chosen from the family of grid generators, developed in the IT AS CR (Jonáš, 1989). The important parameters of grids and the characteristics of generated FST are shown in the Table 1. The following nomenclature was introduced in the Table 1: *d* and *M* are the diameter and the mesh of cylindrical rods; $x_{L.E.}$ signifies the distance of the grid plane from the leading edge of the plate (*x* = 0, the onset of boundary layer); *Iu* (0) and L_e (0) are the intensity and the dissipation length parameter taken after Hancock and Bradshaw (1989)

$$Iu = \sqrt{\overline{\left(u^2\right)}} \Big/ \bar{U}_e; \quad L_e = -\overline{\left(u^2\right)}^{3/2} / \bar{U}_e \frac{\partial \overline{\left(u^2\right)}}{\partial x} \qquad (4)$$

where $\bar{U}_e$ and u are the external flow mean velocity and the longitudinal component of velocity fluctuations. Next the ratio of the integral length scale Λ to L_e , the local (x_1 = 1.2 m) values of the intensity calculated from the decay law $Iu(x_1)$ and measured *exp* $Iu(x_1)$ and the local length parameter evaluated from CTA measurements. It should be mentioned that the generated FST is homogeneous and close to isotropy in plane x = 0.

Table 1 Turbulence generators and characteristics of the generated turbulence (x_1 = 1.2 m).

Grid	*d* [mm]	*M* [mm]	$x_{L.E.}$ *[m]* x = 0	*Iu* (0)	L_e (0) [mm]	Λ/L_e	$Iu(x_1)$	*exp* $Iu(x_1)$	*exp* $L_e(x_1)$
GT0				0.003	~10		0.003	0.003	
GT1	3	20	0.4538	0.030	7.0	1.53	0.011	0.013	17.8
GT3	6	40	1.0697	0.030	12.6	1.29	0.015	0.015	21.0
GT4	6	20	0.7382	0.030	16.2	1.21	0.015	0.015	17.7
GT5	10	35	1.2107	0.030	30.5	1.01	0.020	0.021	36.2
GT8A	1.65	5.75	0.7866	0.010	5.7	1.29	0.005	0.011	12.8
GT8B	1.65	5.75	0.1936	0.030	3.0	2.83	0.007	0.012	12.7
GT8C	1.65	5.75	0.1247	0.050	2.2	2.72	0.007	0.010	10.5
GT9	1	5	0.0925	0.030	0.8	3.37	0.004	0.010	5.2

The measurement of the mean velocity profiles was based on pressure measurements. The Pitot-static tube (diameter = 6 mm) connected with the pressure transducer OMEGA Techn. Ltd., (max 1.2 kPa; ± 0.25% FS) was used for the measurement of the representative dynamic pressure q_r and at the same time for absolute static pressure P_e [Pa] measurement, by means of the pressure transducer Druck DPI 145 (max 100 kPa; ±0.005% FS). Thermometer Pt 100 connected to the Data Acquisition/Switch Unit HP 34970A was applied for the flow temperature *t* [°C] measurement.

The velocity profiles were determined only in the section x = x_1 = 1.2 m from the measurements by means of the couple of the flattened Pitot probe (0.18 x 2.95 mm^2) and round nosed static pressure probe (diameter = 0.18 mm) connected with the pressure transducer BARATRON (special order on high accuracy, max 1 kPa; ±0.02% of reading above 20 Pa). The BARATRON's output signal was proportional to the local dynamic pressure $q'(x,y) = P_0 - P$. Output signals proportional to the mean values of P_e, q_r and *t* were read by means of the unit HP 34970A just after start of measurement-observation in the point [*x, y,* 0] ($z = 0$ is the plane of vertical symmetry of flow). Afterwards the simultaneous reading and 30 s averaging of signals proportional to q_r and $q'(x,y)$ followed. After the end of the reading the data were recorded in a personal computer.

Estimates of upper limits of measurement errors were derived from the accuracy of applied devices and with the regard to the scatter of repeated observations

$$\frac{\Delta q_r}{q_r} \le \pm 0.02 \text{ at } U_r \ge 2.5\, m/s; \quad \frac{\Delta q}{q} \le \pm 0.02 \text{ at } U(x,y) \ge 0.6\, m/s; \quad \Delta P_e \simeq \pm 5\,\text{Pa} \tag{5}$$

The absolute error of the local dynamic pressure at higher local velocity $U(x, y)$ was almost constant, about ± 0.005 Pa, i.e. on the level at $U \approx 0.08$ m/s. More details are given in the former paper Jonáš et al. (2008).

3. Evaluation procedure

The evaluation method is generally discussed in the former paper Jonáš et al. (2008). Here will be described the applied procedure derived with regard to the specific conditions of experiment. The aim of the evaluation of the mean velocity profiles are determination of the coordinate y' corresponding to y = 0, where $\bar{U}(y') = 0$, of the wall shear stress $\tau_w(x)$, the boundary layer thickness, the displacement thickness and the momentum thickness (e.g. Hinze, 1975)

$$\delta\left(\bar{U}(\delta) = 0.99\bar{U}_e\right), \quad \delta_1 \text{ and } \delta_2 \tag{6}$$

Next are evaluated the related characteristics as the shape factor H_{12}, skin friction coefficient C_f and the value of the roughness function Δu^+ and the zero level sink into the layer of roughness elements y_0 more over in the case with rough surface.

The experimental results obtained in cross section $x = 1.2$ m distance from the leading edge of the solid plate with either smooth surface or with the surface covered by sandpaper (grits 80) were affected by the uncertainty of the starting coordinate adjustment. The distances from the wall $y' > 0$ of the probe nose are measured with an accurate cathetometer

$$y'_k = n_k - n_0 + 0.09 \pm 0.02\,[mm] \tag{7}$$

where n_k is the cathetometer observation of the probe nose, n_0 corresponds to the probe position nearest the wall with the first physically reasonable reading of total pressure. The probe traverser's dead travel and elastic deflection of the probe nose are sources of uncertainty of determination the value n_0 just after comes unstuck from the wall or the plane of the roughness spikes. For that reason the evaluation must determine the effective value of the coordinate y'_0 in the case of the smooth surface too. As well, the wall proximity effect on the Pitot tube reading must be corrected. In the first approximation, the first physically reasonable reading is assumed as made in the distance $y'_1 = 0.11\,\text{mm}$. The MacMillan's correction of the total pressure P_o readings (e.g. Tropea et al., 2007) was applied.

Problems of determination the zero level $y' = -y'_0 \le 0$ and the wall shear stress $\tau_w(x)$ are bounded. In case of a turbulent boundary layer are applicable procedures

- Interpolation of the mean velocity profile very near the surface

$$\tau_w(x) = \mu\left(\frac{\partial \bar{U}}{\partial y}\right)_w = \mu\left(\frac{\partial \bar{U}}{\partial y'}\right)_0; \quad \bar{U}(y') = \left(\frac{\partial \bar{U}}{\partial y}\right)_w (y' + y_0'); \quad y' = O(10^{-4}m) \qquad (8)$$

the magnitude of y_0' is searching giving the best fit of (8).

- Interpolation of the log-law that can be written in the form

$$\frac{\bar{U}}{u_\tau} = \frac{1}{\kappa} ln\left(y^+\right) + B - \Delta u^+\left(s^+\right); \quad y^+ = \frac{y\,u_\tau}{\nu} \qquad (9)$$

where $\kappa = 0.41$ and $B = 5$ are the von Kármán constant and the smooth wall log-law intercept. The function of the roughness, Δu^+, expresses the shift of the velocity semi-logarithmic plot below the shape in case of aerodynamically smooth surface. Once the roughness function was determined for the given surface it can be used for the friction loses calculations of any surface with the same roughness, Rotta (1972). The log-law deviates from the actual velocity profile for large values of y^+ then the formula (9) does not hold above the inertial sub-layer. So the velocity defect is more appropriate

$$\frac{\bar{U}_e - \bar{U}(y)}{u_\tau} = -\frac{1}{\kappa} ln\left(\frac{y}{\delta}\right) + B_2\left(\frac{u_\tau}{\bar{U}_e}\right) \qquad (10)$$

From Clauser (1954) investigations results, that for $y/\delta < 0.15$ the approximation

$$\frac{\bar{U}_e - \bar{U}(y)}{u_\tau} = -\frac{1}{\kappa} ln\left(\frac{y}{\delta}\right) + 2.5 \qquad (11)$$

is valid with a small scattering (e.g. Hinze, 1975 and Rotta, 1962). This formulae is lending an assistance for the evaluation of the three unknowns $y_0', u_\tau, \Delta u^+$. Beyond the distance $y/\delta \sim 0.15$ the difference between the actual velocity profile in the outer layer and the log-law is called the wake function. Hancock (1980) proved that the wake function depends on the external turbulence characteristics. He did not found a satisfactory formulation for a wake function in an external turbulent flow. So the approximation (11) was assumed for the presented study together with the Hama (1954) empirical formula for the mean velocity profile in the outer part of boundary layer

$$\frac{\bar{U}_e - \bar{U}(y)}{u_\tau} = C\left(1 - \frac{y}{\delta}\right)^2; \quad y > 0.15\,\delta \qquad (12)$$

Let us make two useful remarks to this discussion that follow from the above-mentioned papers and the personal experience. With increasing roughness is decreasing the thickness of viscous sub-layer and the upper bound of the log-law validity region is moving away from the wall. Thus the log-law region – the inertial sub-layer - is expanding with increasing wall roughness.

The evaluation of the three unknowns $y_0', u_\tau, \Delta u^+$ is executed by means the equation (9) rearranged in the form

$$\frac{\bar{U}}{\bar{U}_e} = a\, ln\left(\frac{(y' + y_0')\bar{U}_e}{\nu}\right) + b \qquad (13)$$

The task is: interpolate this regression function in the region of the log-law validity (in the 1st approximation: ~30 < y^+ < ~750) and determine parameters a, b and y'_0 so as

1) the correlation coefficient became maximum (canonical definition of r^2);

and simultaneously are fulfilled requirements:

2) closely to the surface the relation $min\,u^+ \leq y^+$;

3) at the outer bound of log region and little further several points of measurement approach the distribution (11).

Afterwards are derived the remaining unknowns $u_\tau, \Delta u^+$

$$\frac{u_\tau}{\bar{U}_e} = \kappa a; \quad \Delta u^+ = \frac{1}{\kappa} ln\left(\frac{u_\tau}{\bar{U}_e}\right) + B - \frac{1}{\kappa}\frac{b}{a} \tag{14}$$

Few times we succeeded apply both procedures the one based on (8) and the other on (13). The differences were less than 10 percent.

4. Results

Experiments with smooth wall were evaluated first of all. It has been ascertained that due to the problem with the probe traverser's dead travel and elastic deflection of the probe nose the actual mean velocity zero level was at the coordinate

$$(y')_{smooth} = -0.187 \text{ mm } \pm 0.036 \text{ mm} \tag{15}$$

This value is the average from coordinates derived together with interpolating turbulent boundary profiles by log-law. An example of results at the momentum thickness Reynolds number Re_2 =2200 is shown in the Figure 1.

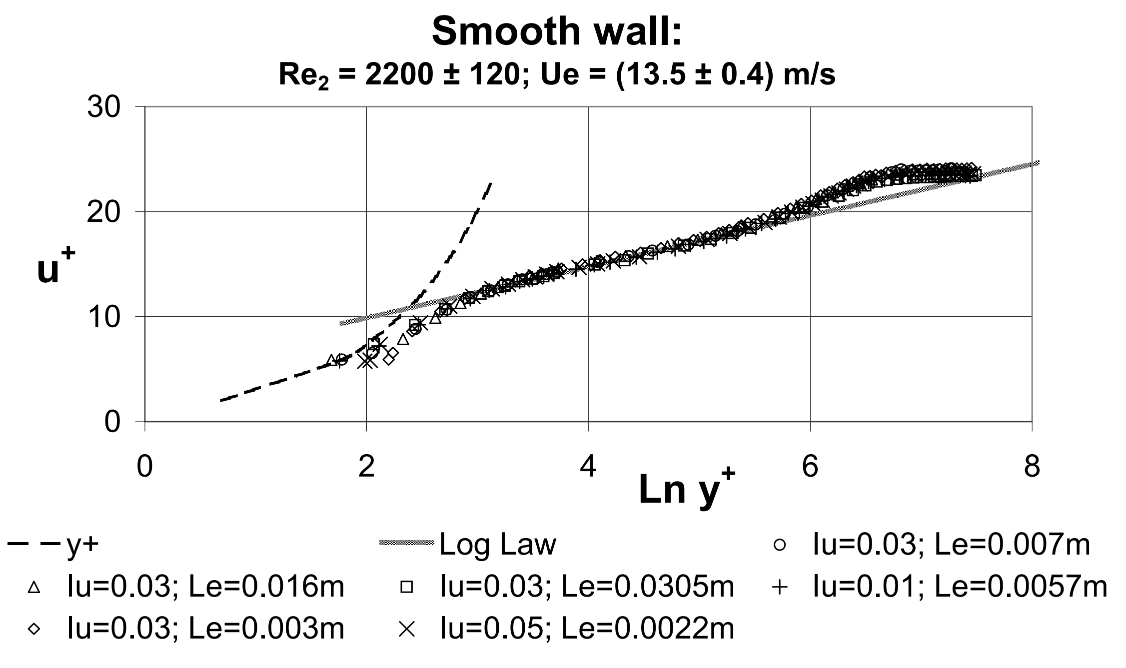

Figure 1 An example of results at the momentum thickness Reynolds number Re2 = 2200

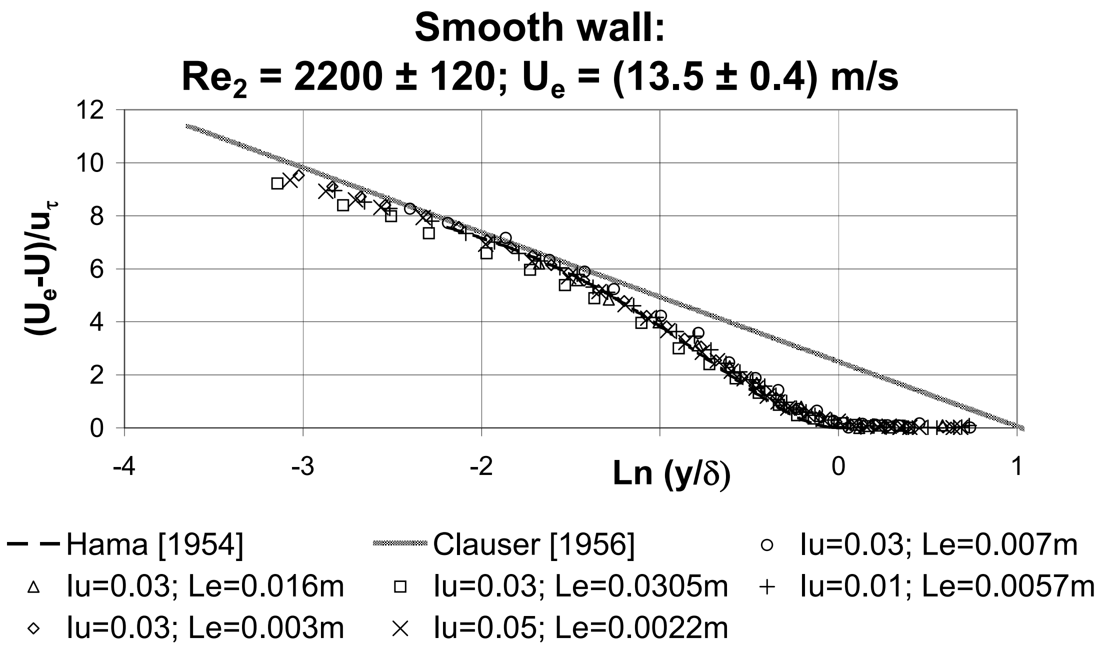

Figure 2 Velocity defect fit corresponding to the Reynolds number Re_2 =2200

In the Figure 2 is shown the corresponding velocity defect fit. The effect of external flow turbulence characteristics is obvious on the velocity defect. This result is in accord with published papers e.g Hancock (1980).

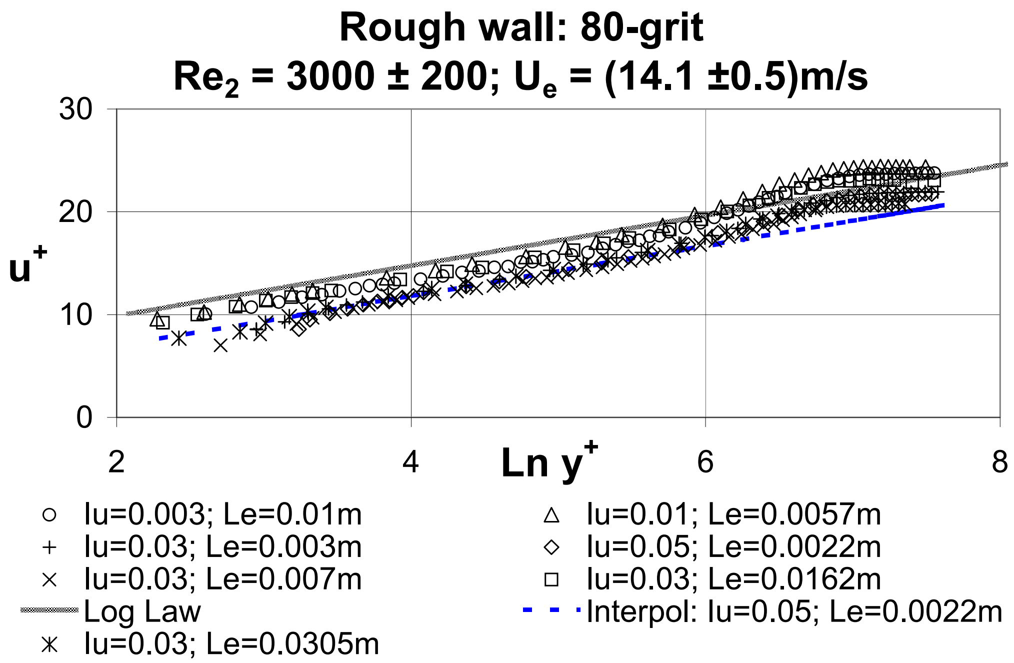

Figure 3 The role of the roughness function Δu^+ (9)

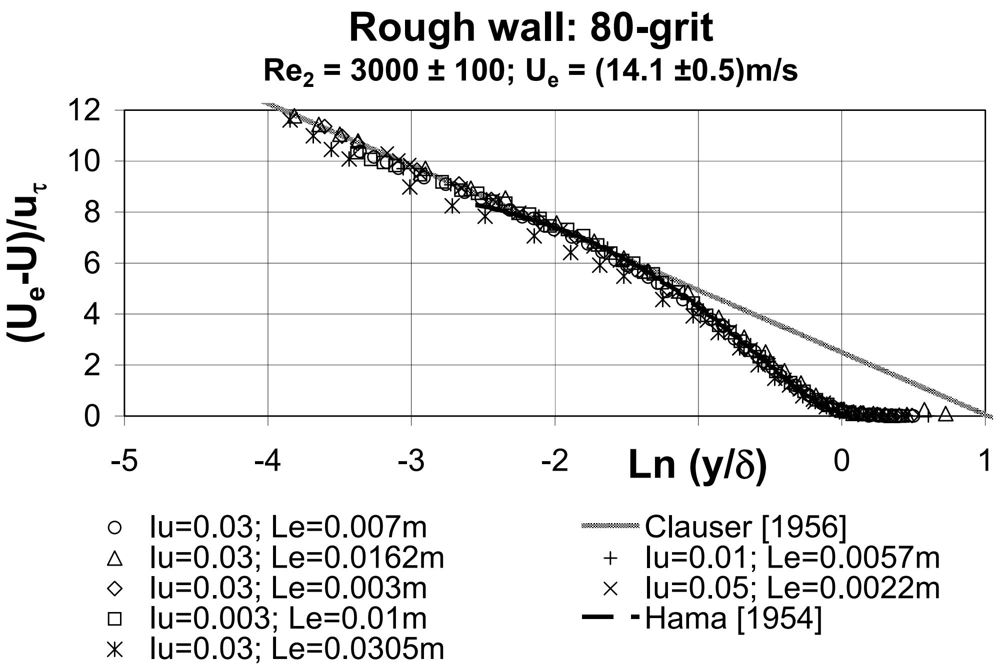

Figure 4 Velocity defect fit corresponding to the Reynolds number Re_2 =3000
Rough wall: 80-grit

Similarly the evaluation of measurements with the rough plate started. The coordinate of the zero level was ascertained as the average from all performed interpolations of log-law

$$(y')_{rough} = -0.314 \text{ mm } \pm 0.065 \text{ mm} \qquad (16)$$

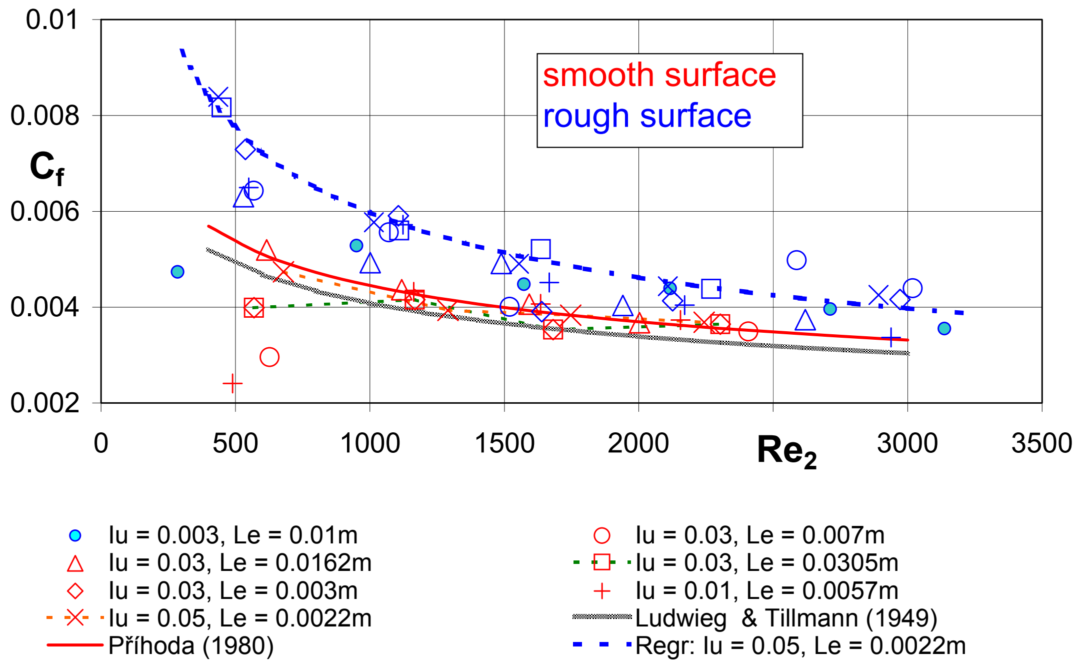

Figure 5 Distributions of the skin friction coefficient C_f

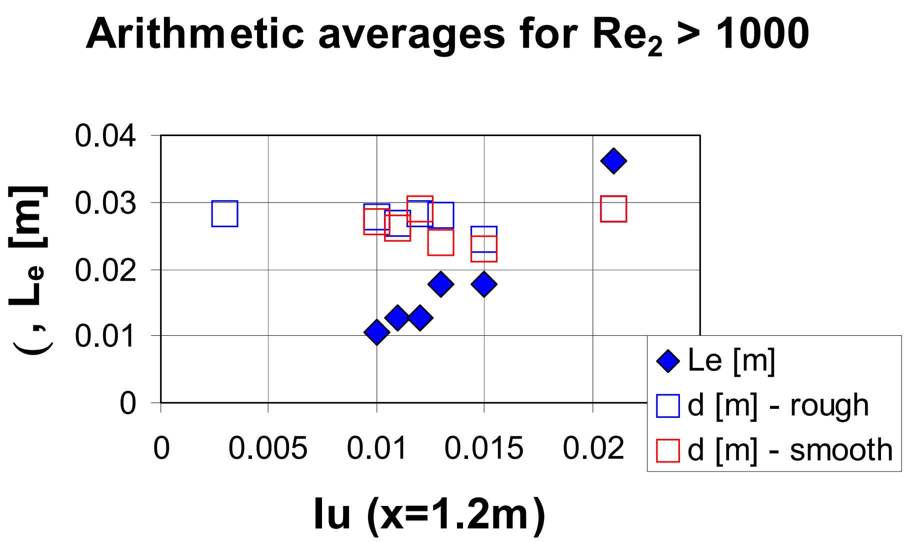

Figure 6: Arithmetic averages for Re_2>1000 versus the intensity *Iu* of external turbulence in the leading edge plane, $x = 0$

Having in mind that this value includes also the shift (15) we concluded that the velocity zero level is about 0.127 mm below the top plane of the roughness elements (s = 0.343 mm). It seems like useless keep in mind such small and with a great scatter derived quantity in the interpolation of log-law. However to do it is necessary in order to reach a satisfactory results

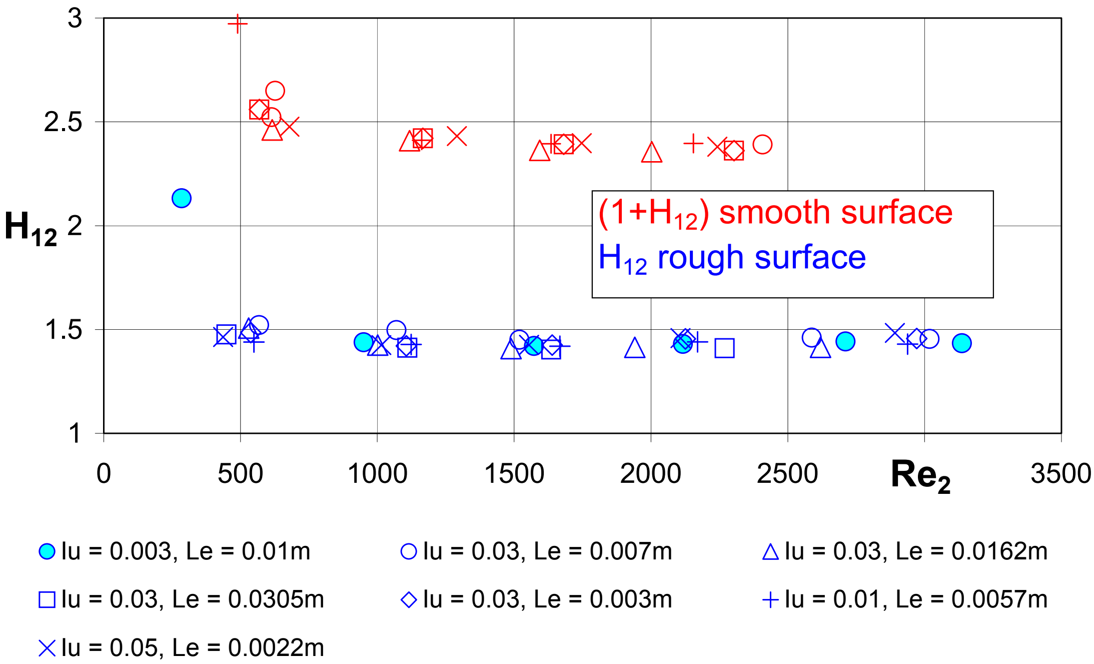

Figure 7 The shape factor H_{12} as a function of Reynolds number Re_2.

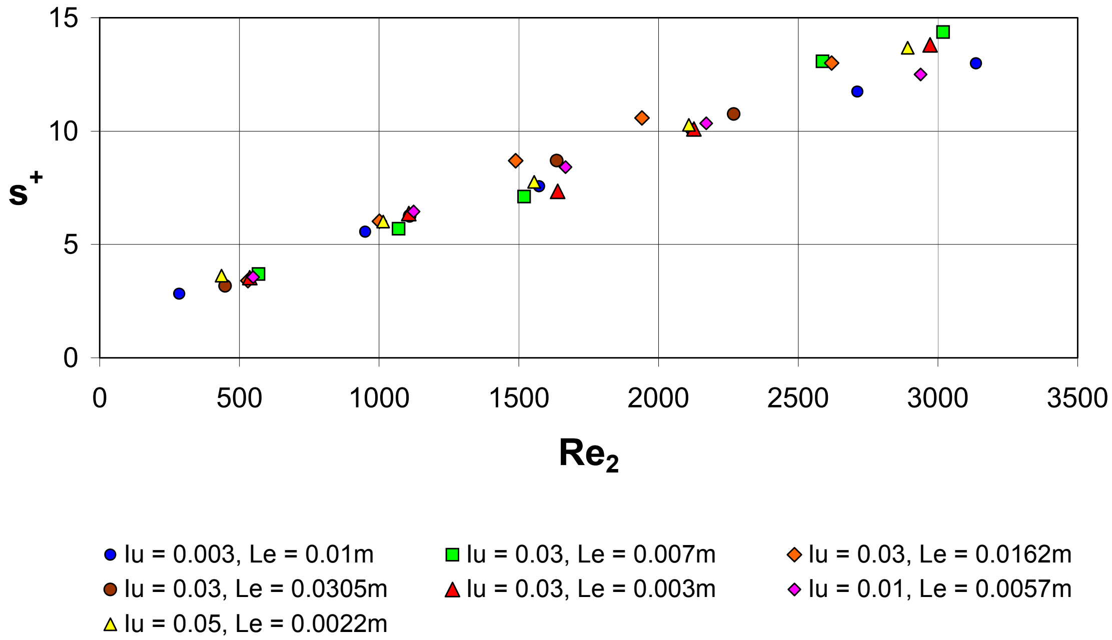

Figure 8 The distribution of the surface roughness parameter s^+ (1) versus Re_2

e.g. Figure 3 and 4. The Figure 3 demonstrates the role of the roughness function Δu^+ (9) that will be discussed later. The effect on turbulent boundary layers of the surface roughness is more weighty than the effect of external flow turbulence $[Iu, L_e]_e$ as follows from the Figures 1 and 3. The comparison of Figures 2 and 4 indicate that the deviations from the velocity defect formulae, known as a result of external turbulence, are smaller when the surface is rough. This conclusion is more apparent from the distributions of the skin friction coefficient C_f in Figure 5. Together with the experimental results, are plotted in the Figure 5: the

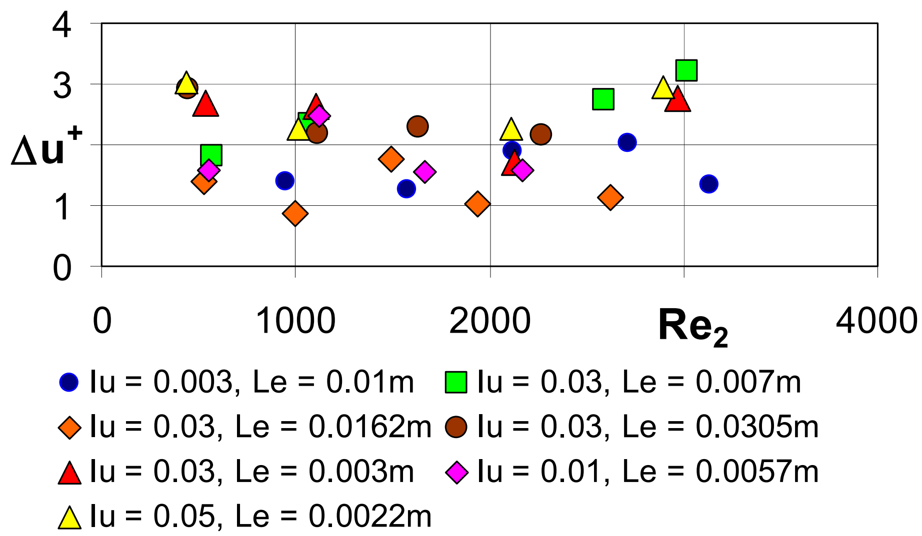

Figure 9 The received measurements results indicate no apparent dependence on Reynolds number in the investigated region of the *transitional roughness* up to about $Re_2 = 3000$.

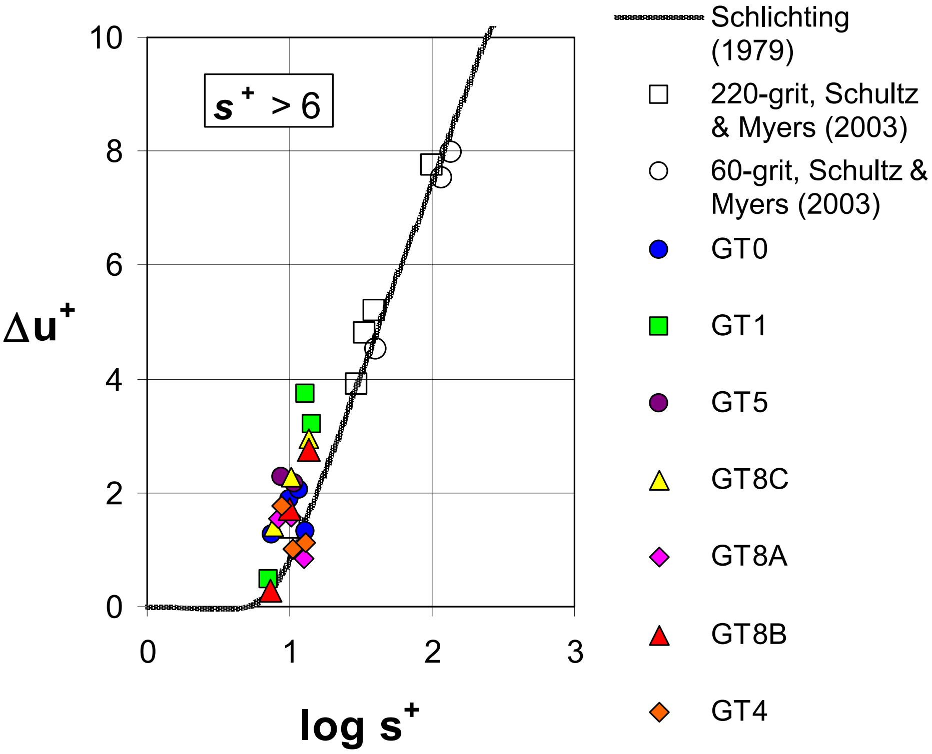

Figure 10 A comparison of the presented results with the Nikuradse-type roughness function for uniform sand given by Schlichting (1979) and with the results obtained by Schultz and Myers (2003)

Ludwieg-Tillmann (1949) formulae, the empirical forecast of the gain in skin friction done by external turbulence after Příhoda (1980) and finally an example of regression of measurement is shown.

The thicknesses of boundary layers are derived in a customary way applying the knowledge of individual quantities y_0' describing zero levels of mean velocity (values (15) and (16) are their averages). Apparently, the thickness δ (measured from the *zero level*) only mildly depends on the local turbulence intensity and roughness of the surface, Figure 6.

The shape factor H_{12} is shown in the Figure 7 as a function of Reynolds number Re_2. The average values 1.41 (smooth surface) and 1.43 (rough surface) are very close for $Re_2 > 1000$ and do not depend on external flow turbulence characteristics. Obviously turbulent boundary layers were developed at $Re_2 > 1000$.

The distribution of the surface roughness parameter s^+ (1) versus Re_2 (Figure 8) demonstrates that the roughness of the plate covered with sandpaper belongs to the category of *transitional roughness* only if the momentum thickness Reynolds number exceeds thousand, $\mathrm{Re}_2 > 1000$.

The function of the roughness Δu^+ is describing the shift of the semi-logarithmic plot of the mean velocity profile on rough surface below the log law in case of aerodynamically smooth surface, e.g. Figure 3. The received measurements results, Figure 9, indicate no apparent dependence on Reynolds number in the investigated region of the *transitional roughness* up to about $\mathrm{Re}_2 = 3000$.

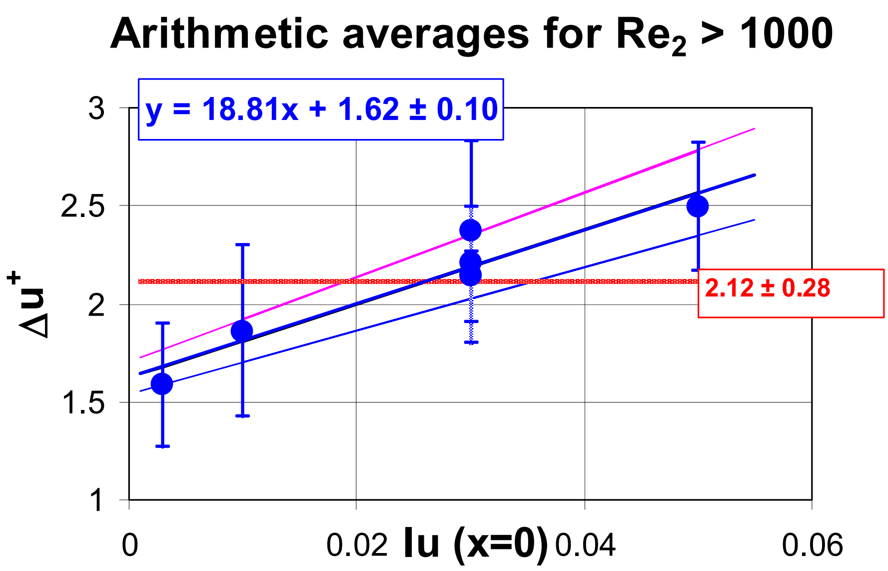

Figure 11 The arithmetic averages and the corresponding standard deviations versus the intensity *Iu* of external turbulence in the leading edge plane, $x = 0$.

A comparison of the presented results with the Nikuradse-type roughness function for uniform sand given by Schlichting (1979) and with the results obtained by Schultz and Myers (2003) is shown in the Figure 10. The results follow the course of the Nikuradse-type roughness function. They would follow with an acceptable scatter the curve after increasing the roughness representative length *s* by 20 percent.

Seeking to improve clearness of some subsequent analyses, the averages of the roughness function at various Re_2 were calculated for each individual regime of external turbulence. The averages and the corresponding standard deviations (from 2 percent up to 23 percent with the

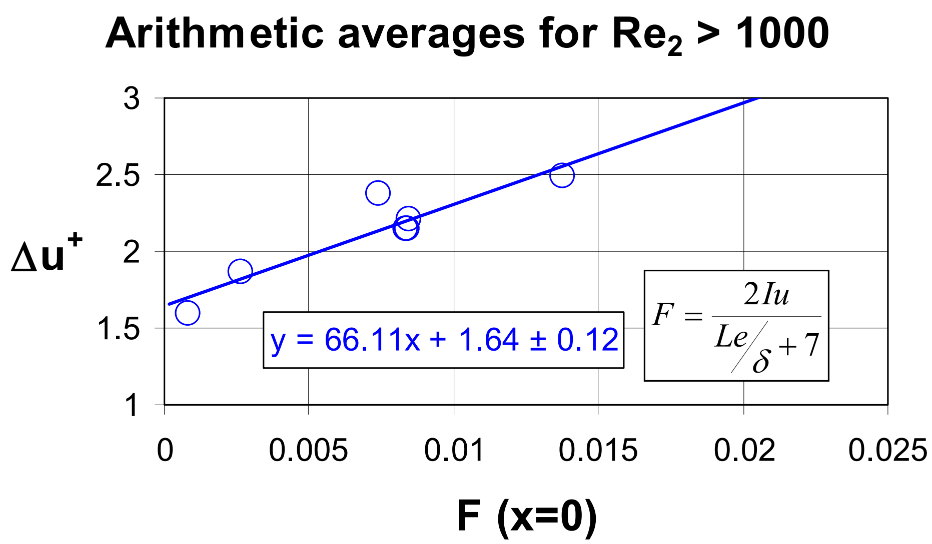

Figure 12 Arithmetic averages for Re_2>1000 versus external turbulence parameter F

mean 15 percent) are shown in the Figure 11 versus the intensity *Iu* of external turbulence in the leading edge plane, x = 0. The average of all plotted values of Δu^+ is equal 2.12 ± 0.28 (red line). The roughness function Δu^+ is an increasing function of the intensity *Iu*

$$\Delta u^+ = 1.62 + 18.81\, Iu(0) \quad \pm 0.10 \tag{17}$$

The small relative probable error of this interpolation is about 5%. This result must be taken very carefully because it cannot be overlooked that it follows from averaged quantities with a big scatter (about 13 percent).

The effect of external flow turbulence length scale on the function Δu^+ was not proved as shown in the Figure 12. Features of the external turbulence were characterized by the parameter including the intensity *Iu* and then the dissipation length parameter L_e and the boundary layer thickness δ

$$F(x) = \frac{2Iu}{L_e/\delta + 7} \tag{18}$$

This parameter was introduced in analogy to Hancock and Bradshaw (1983), see as well Jonáš (1992). The regression

$$\Delta u^+ = 1.64 + 66.11\, F(0) \quad \pm 0.12 \tag{19}$$

with the value F at x = 0 appears slightly less statistically fitting than the regression (17).

Variations of the roughness function Δu^+ with the local values of intensity *Iu* or parameter F were also analyzed. However no systematic dependences were found.

6. Conclusions

The effect on turbulent boundary layers of the surface roughness is more weighty than the effect of external flow turbulence characteristics. The deviations from the velocity defect formulae, known as a result of external turbulence, are reduced when the surface is rough. This conclusion is apparent from the mean velocity profiles and from the distributions of the skin friction coefficient C_f in Figure 5.

The velocity zero level is about 0.127 mm below the top plane of the roughness elements (s = 0.343 mm).

The boundary layer thickness δ (measured from the *zero level*) and the shape factor H_{12} are only mildly affected by the individual and joint effect of the local turbulence intensity and the roughness of the surface.

The distribution of the surface roughness parameter s^+ versus Re_2 demonstrates that the roughness of the plate covered with sandpaper belongs to the category of *transitional roughness* only if the momentum thickness Reynolds number exceeds thousand, $Re_2 > 1000$. Otherwise the flow was developing near the hydraulically smooth surface regime.

No apparent dependence of the roughness function Δu^+ was found on Reynolds number in the investigated region of the *transitional roughness* up to about Re_2 = 3000. Thus the averages of the roughness function at various Re_2 were calculated for each individual regime of external turbulence and analyzed. The results follow the course of the Nikuradse-type roughness function for uniform sand. They would fit, with an acceptable scatter, the curve after introducing the roughness representative length *s* increased by 20 percent. The value of the roughness function increases with external turbulence intensification which describe empirical formulas (17) and (19).

The evaluation procedure was developed that allows determine all unknowns $y_0', u_\tau, \Delta u^+$ from the mean velocity profile with estimates of the probable relative errors about 0.2, 0.05, 0.13 respectively.

7. Acknowledgement

The Grant Agency of the Academy of Sciences of the Czech Republic, project no. A200760614, supported this work.

8. References

Clauser, F.H (1954) Turbulent boundary layers in adverse pressure gradients. Advances in Appl. Mechanics, 4, 1

Hama, F.R. (1954) Boundary layer characteristics for smooth and rough surfaces. Trans. Soc. Naval Architects Marine Engrs. 62,333-358.

Hancock, P.E. (1980) *The effect of free stream turbulence on turbulent boundary layer*. PhD. –Thesis, Imperial College, University of London.

Hancock, P.E. and Bradshaw, P. (1983) The effect of free stream turbulence on turbulent boundary layers. Trans. ASME, J. of Fluid Engng., 105, 287-289.

Hinze, J.O. (1975) *Turbulence*. McGraw-Hill, New York (2. ed.).

Jonáš, P. (1989) Control of free stream turbulence by means of passive devices. In: Proc. Of International Seminar "Problems of simulation in wind tunnels". Pt.2 ITPM SO AN SSSR, Novosibirsk, 160-174.

Jonáš, P. (1992) On turbulent boundary layer perturbed by outer flow turbulence. Energetika Nr. 3 (ISSN 0235-7208), Vilnius, Latvia, 69-80.

Jonáš, P. (2008) Mean velocity profiles in a boundary layer under the joint action of surface roughness and external turbulent flow. Applied and Computational Mechanics 2, 273-284.

Jonáš, P., Mazur, O. and Uruba, V. (2000) On the receptivity of the by-pass transition to the length scale of the outer stream turbulence. Eur. J. Mech. B – Fluids 19, 707-722.

Jonáš, P., Mazur, O. and Uruba, V. (2008) Preliminary study on the effect of the wall roughness and free stream turbulence on the boundary layer development. Proc. Conf. Engineering Mechanics 2008, Institute of Thermomechanics, Academy of Sciences of the Czech Republic, v.v.i., Prague, ISBN 978-80-87012-11-6, CD ROM, 1-13.

Kline, S.J., Cantwell, B.J. and Lilley, G.M. (1980) *Complex turbulent flows*. Proc. Of the 1980 Conference, Stanford University, Sept. 3-6, Stanford, California.

Pope, S. B. (2000) *Turbulent flows*. Cambridge University Press, Cambridge.

Příhoda, J. (1980) The effect of the external flow turbulence intensity on parameters of a turbulent boundary layer /in Czech). Strojnický Časopis 31, č. 5, 649-659.

Rotta, J. C. (1962) Turbulent boundary layer in incompressible flow, in: *Progress in Aeronautical Sciences* (A. Ferri, D. Küchemann & L. H. G. Sterne eds.) Pergamon Press, Oxford, pp. 1-220.

Rotta, J.C. (1972) *Turbulente Strömungen*. B.G. Teubner, Stuttgart.

Schultz, M.P. and Myers, A. (2003) Comparison of three roughness function determination methods. Experiments in Fluids 35, 372-379

Schlichting, H. (1979) *Boundary Layer Theory*. .7th edn. McGraw-Hill, New York.

Schlichting, H. & Gersten, K. (2000) *Boundary-Layer Theory*. Springer, Berlin.

Tropea, C., Yarin, A. L. & Foss, J. F. (Eds.) (2007) *Springer Handbook of Experimental Fluid mechanics.* Springer-Verlag Berlin.